

DELPHI Collaboration

DELPHI 2002-039 CONF 573  
27 June, 2002

---

## Search for Doubly Charged Higgs Bosons at LEP2

G. Gómez-Ceballos<sup>1</sup> and F. Matorras<sup>1</sup><sup>1</sup>Instituto de Física de Cantabria (CSIC-UC), Santander, Spain

### Abstract

A search for pair-produced doubly charged Higgs bosons has been performed using the data collected by the DELPHI detector at LEP at centre-of-mass energies between 189 and 209 GeV. No excess is observed in the data with respect to the Standard Model background. A lower limit for the mass of  $97.3 \text{ GeV}/c^2$  at the 95% confidence level has been set for doubly charged Higgs bosons in left-right symmetric models for any value of the Yukawa coupling between the Higgs bosons and the  $\tau$  leptons.

Contributed Paper for ICHEP 2002 (Amsterdam)

# 1 Introduction

Doubly charged Higgs bosons ( $H^{\pm\pm}$ ) appear in several extensions to the Standard Model [1], such as left-right symmetric models, and can be relatively light. For example, they can lead to small neutrino masses. In Supersymmetric left-right models usually the  $SU(2)_R$  gauge symmetry is broken by two triplet Higgs fields, so-called left and right handed. Pair-production of doubly charged Higgs bosons is expected to occur mainly via  $s$ -channel exchange of a photon or a  $Z$  boson. In left-right symmetric models the cross-section of  $e^+e^- \rightarrow H_L^{++}H_L^{--}$  is different from that for  $e^+e^- \rightarrow H_R^{++}H_R^{--}$ , where  $H_L^{\pm\pm}$  and  $H_R^{\pm\pm}$  are the left-handed and right-handed Higgs bosons. The formulae for the decays and the production of these particles can be found in [2].

In these models the doubly charged Higgs couples only to charged lepton pairs, other Higgs bosons, and gauge bosons, at the tree level. The current limit and the mass range of this analysis is restricted to the interval between 45 GeV/ $c^2$ , the LEP1 limit set by OPAL [3], and the kinematic limit at LEP2, that is around 104 GeV/ $c^2$ . The dominant decay mode of the doubly charged Higgs boson is expected to be a same sign charged lepton pair, the decay proceeding via a lepton number violating coupling. As discussed in [2], due to limits that exist for the couplings of  $H^{\pm\pm} \rightarrow e^\pm e^\pm$  from high energy Bhabha scattering,  $H^{\pm\pm} \rightarrow \mu^\pm \mu^\pm$  from the absence of muonium to anti-muonium transitions and  $H^{\pm\pm} \rightarrow \mu^\pm e^\pm$  from limits on the flavour changing decay  $\mu^\pm \rightarrow e^\mp e^\pm e^\pm$ , electron and muon decays are not likely. In addition, most of the models expect that the coupling to  $\tau\tau$  will be much larger than any of the others. Therefore, only the doubly charged Higgs boson decay  $H^{\pm\pm} \rightarrow \tau^\pm \tau^\pm$  is considered here.

The partial width for the  $H^{\pm\pm}$  decay into two  $\tau$  leptons is, at the tree level [2]:

$$\Gamma_{\tau\tau}(H^{\pm\pm} \rightarrow \tau^\pm \tau^\pm) = \frac{h_{\tau\tau}^2}{8\pi} m_H \left(1 - \frac{2m_\tau^2}{m_H^2}\right) \left(1 - \frac{4m_\tau^2}{m_H^2}\right)^{1/2} \quad (1)$$

where  $m_\tau$  is the mass of the  $\tau$  lepton and  $h_{\tau\tau}$  is the unknown  $H\tau\tau$  Yukawa coupling constant. Depending on the  $h_{\tau\tau}$  coupling and the Higgs mass the experimental signature is different. If  $h_{\tau\tau}$  is sufficiently large,  $h_{\tau\tau} \geq 10^{-7}$ , the Higgs decays very close to the interaction point. We describe here an analysis to search for such events. If  $h_{\tau\tau}$  is smaller the decay occurs inside the tracking detectors or even beyond them, making this analysis inefficient. In this case pre-existing analyses were applied which are further discussed below.

## 2 Data sample and event generators

The data collected by DELPHI during the LEP runs at centre-of-mass energies from 189 GeV to 209 GeV were used. The total integrated luminosity of these data samples is  $\sim 570$  pb $^{-1}$ . The DELPHI detector and its performance have already been described in detail elsewhere [4, 5].

Signal samples were simulated using the PYTHIA generator [6]. In this analysis samples with doubly charged Higgs boson with masses between 50 and 100 GeV/ $c^2$ , in 10 GeV/ $c^2$  steps, were used at different centre-of-mass energies, both for left-handed and right-handed bosons, and different Yukawa coupling constants.

The background estimates from the different Standard Model processes were based on the following event generators, interfaced with the full DELPHI simulation program [5]. The WPHACT [7] generator was used to produce four fermion Monte-Carlo simulation events. The four-fermion samples were complemented with dedicated two-photon collision samples generated with BDK, BDKRC [8] and PYTHIA [6]. Samples of  $q\bar{q}(\gamma)$  and  $\mu^+\mu^-(\gamma)$  events were simulated with the KK2f generator [9]. Finally, KORALZ [10] was used to simulate  $\tau^+\tau^-(\gamma)$  events and the generator BHWIDE [11] was used for  $e^+e^-(\gamma)$  events.

### 3 Data selection

The search for pair-produced doubly charged Higgs bosons makes use of three different analyses depending on the  $h_{\tau\tau}$  coupling or, equivalently, on the mean decay length of the doubly charged Higgs boson. When the mean decay length of the Higgs boson is very small, the resulting final state consists of four narrow and low multiplicity jets coming from the interaction point. This analysis will be explained in detail in section 3.1. For intermediate mean decay lengths of the Higgs the topology consists of two tracks coming from the interaction point and either secondary vertices or kinked tracks. If the Higgs decays outside the tracking devices the signature corresponds to stable heavy massive particles. Details of these last two analyses can be found in [12].

#### 3.1 Small impact parameter search

An initial set of cuts was applied to select events with four jets of low multiplicity. Only tracks with an impact parameter below 4 cm both in the plane transverse to the beam pipe and in the direction along the beam pipe were considered in the analysis. A charged particle multiplicity between 4 and 8 was required. Events were clustered into jets, requiring each jet to be separated from the others by at least 15 degrees, and only events with four reconstructed jets were accepted. To improve the reconstruction of the tau energy, the tau momenta were rescaled, imposing energy and momentum conservation and keeping the tau directions at their measured values. Events with any negative rescaled momentum were rejected as they are commonly not genuine four-jet events.

In order to reduce the two-photon background the following energy and momentum requirements were applied: the visible energy outside a cone of  $25^\circ$  around the beam had to be greater than  $0.15\sqrt{s}$ , the momenta of the jets were required to be larger than  $0.01\sqrt{s}$  and the total neutral energy had to be less than  $0.35\sqrt{s}$ .

The four lepton background was rejected by requiring that the momentum of the most energetic lepton identified (electron or muon) was less than  $0.25\sqrt{s}$  and the momentum of the second most energetic lepton identified was less than  $0.15\sqrt{s}$ . The algorithms used in the lepton identification were the same as those used in the selection of fully-leptonic  $W$  pairs in DELPHI data [13].

The calculated tau momenta, defined above, were used to reconstruct the Higgs mass. The charge of the tau jet was calculated as the sum of the charges of the charged particles in the jet. If this value was not  $\pm 1$ , then the charge of the most energetic charged particle was assumed as to be the charge of the tau jet. For events with two positive  $\tau$  lepton candidates and two negative  $\tau$  lepton candidates the charge was used to assign

the pairing of both doubly charged Higgs bosons. If the total charge was not equal to 0, the pairing into two di-jets was chosen as that which minimizes the difference between the reconstructed masses of the di-jets. The ratio  $\frac{|M_{H^{++}} - M_{H^{--}}|}{(M_{H^{++}} + M_{H^{--}})/2}$  was required to be less than 0.7. Finally the reconstructed event mass, defined as the average of the mass of the two pairings, had to be greater than  $40 \text{ GeV}/c^2$ . The reconstructed event mass was used as an additional discriminant variable in the computation of the confidence levels.

The effects of the selection cuts are shown in Table 1 for the combined 189-208 GeV sample. After all cuts were applied only one event was observed in the data with a mass of  $69 \pm 3 \text{ GeV}/c^2$ , while 0.9 events were expected from background processes. The candidate was collected at  $\sqrt{s}=206.7 \text{ GeV}$  and is compatible with the assignment  $ZZ \rightarrow \tau^+\tau^-\tau^+\tau^-$ . The most probable reconstructed masses with different sign leptons are indeed compatible with a  $M_Z$ - $M_Z$  mass hypothesis at the one sigma level. The signal efficiency was around 40% for a wide range of masses between 70 and  $100 \text{ GeV}/c^2$  for both left-handed and right-handed doubly charged Higgs, as shown in Table 2. Table 3 shows the selection efficiencies for left-handed doubly charged Higgs bosons for several  $H^{\pm\pm}$  masses and several  $h_{\tau\tau}$  couplings at  $\sqrt{s}=206.7 \text{ GeV}$ . The final reconstructed mass spectrum and the expected mass distribution in simulated signal events are shown in Figure 1. The good level of agreement between data and simulation observed at different stages of the analysis is demonstrated in Figure 2.

cut	data	total bkg.	$llll$	other	$\varepsilon_{H_L^{++}H_L^{--}}$
Four jets preselection	59	$67.4 \pm 0.95$	44.0	23.4	59.2%
anti $\gamma\gamma$ cuts	26	$31.0 \pm 0.48$	28.9	2.1	52.3%
anti 4 lepton cuts	1	$1.9 \pm 0.07$	1.7	0.2	48.7%
Mass requirements	1	$0.9 \pm 0.05$	0.8	0.1	44.2%

Table 1: The total number of events observed and the expected background after the different cuts used in the analysis for the small impact parameter search for the combined 189-208 GeV sample. The last column shows the efficiency for a left-handed doubly charged Higgs boson signal with  $m_{H_L^{\pm\pm}} = 100 \text{ GeV}/c^2$  at  $\sqrt{s}=206.7 \text{ GeV}$ .

channel	$M_{H^{\pm\pm}} \text{ (GeV}/c^2)$					
	50	60	70	80	90	100
left-handed	32.7	36.6	40.5	44.8	43.4	44.2
right-handed	31.8	37.0	40.0	44.0	44.8	45.2

Table 2: Selection efficiencies (in %) for left-handed and right-handed  $H^{++}H^{--} \rightarrow \tau^+\tau^+\tau^-\tau^-$  for several  $H^{\pm\pm}$  masses and  $h_{\tau\tau} \geq 10^{-7}$  at  $\sqrt{s}=206.7 \text{ GeV}$ , for the small impact parameter search. The statistical error is around 1.5% in all cases.

### 3.1.1 Systematic uncertainties

Several sources of uncertainties on signal efficiencies and background rates were investigated. The particle identification was checked on di-lepton samples both at the Z peak

$h_{\tau\tau}$	$M_{H^{\pm\pm}}$ (GeV/ $c^2$ )			
	50	70	90	100
$4 \cdot 10^{-8}$	0.2/38.1/13.1	1.6/43.0/1.4	6.0/23.9/0.0	20.5/5.3/0.0
$10^{-8}$	0.0/6.4/68.4	0.0/16.0/57.2	0.0/30.5/22.7	0.0/36.3/7.3
$\leq 10^{-9}$	0.0/0.0/77.6	0.0/0.0/77.6	0.0/0.0/41.3	0.0/0.0/41.6

Table 3: Selection efficiencies (in %) for left-handed doubly charged Higgs bosons for several  $H^{\pm\pm}$  masses and several  $h_{\tau\tau}$  at  $\sqrt{s}=206.7$  GeV couplings, for the three analyses performed (small impact parameter search, search for secondary vertices or kinks and search for stable massive particles respectively). The statistical error is around 1.5% in all cases.

and at high energy. The discrepancy on the efficiencies between the data and the simulation were found to be lower than 2% in all cases. The track selection and the track reconstruction efficiency was also studied with these samples. These effects were studied by the comparison between data and simulation at the boundaries of sub-detectors. The systematic error of these effects was about 1.5%.

The errors on the background and signal rates from the modelling of the preselection variables and the detector response were a few percent. Different variables at preselection level have been studied, with good agreement between data and simulation observed. The distributions in relevant variables before the anti- $\gamma\gamma$  cuts and the anti-four-lepton cuts are shown in Figure 2. The masses reconstructed from both same sign and different sign lepton pairs, before the anti-four-lepton cuts were applied, are shown in Figure 3. For the opposite sign lepton pairs only the mass of the combination closest to the Z mass has been given and the Z peak is clearly visible.

The dominant part of the background uncertainty ( $\sim 12\%$ ) is due to the limited simulation statistics available. The total systematic error on the background is about 13%. The total systematic error on the efficiency is about 5%.

### 3.2 Search for secondary vertices or kinks

When the lifetime is such that the particle decays inside the tracking detector, the previous analysis is inefficient, because impact parameter cuts are applied to reject the background coming from secondary interactions. We have applied here the analysis described in [12], that performs a special track reconstruction for this particular topology, looking for decay vertices far from the interaction point.

After all cuts 5 events were selected in the data, while 2.9 events were expected from the background. The signal efficiency was  $\sim 40\%$ , if the mean decay length was  $\sim 50$  cm with a smooth fall for both lower and higher mean decay lengths. The selection efficiencies for several  $H^{\pm\pm}$  masses and several  $h_{\tau\tau}$  couplings at  $\sqrt{s}=206.7$  GeV are shown in Table 3.

### 3.3 Search for stable massive particles

If the lifetime is larger, the  $H^{\pm\pm}$  crosses the tracking devices without decaying. The analysis described in [12] to search for stable heavy particles is applied here. It is based on

the measurement of anomalous ionisation loss measured in the Time Projection Chamber and of the Cherenkov light detected in the Ring Imaging Cherenkov Detector.

One event was selected in the data, in agreement with the expected background of 1.9 events. For stable particle masses in the range of 50-80 GeV/ $c^2$  the efficiency was  $\sim 75\%$ , decreasing to  $\sim 40\%$  for masses near the kinematic limit (Table 3).

## 4 Determination of the mass limit

No evidence for  $H^{++}H^{--}$  production was observed. A likelihood ratio technique [14] has been used to compute the cross-section and mass limits. The reconstructed event mass was used as a discriminant variable in the computation of the confidence levels in the small impact parameter analysis. All centre-of-mass energies and the three analyses were treated as independent experiments in the likelihood function. For intermediate mean decay lengths of the Higgs, due to the exponential decay law, in many cases two analyses have significant efficiency. However the overlap of the samples selected by the analyses, both for the signal and for the background, was negligible.

A very similar behaviour, both in terms of efficiency and of mass distributions, was observed for the left-handed and the right-handed doubly charged Higgs bosons. Hence, the average of both contributions were used to calculate the confidence levels. The expected left-handed and right-handed cross-sections were calculated using the PYTHIA generator [6].

Previous searches for  $H^{\pm\pm}$  pair production have already excluded  $M_{H^{\pm\pm}} < 45.6$  GeV/ $c^2$  [3]. Therefore, we have limited this search to masses greater than this value. The limits at 95% confidence level for different values of  $h_{\tau\tau}$  are shown in table 4. Figure 4 shows the 95% confidence level upper limits on the cross-section at  $\sqrt{s} = 206.7$  GeV for the production of  $H^{++}H^{--} \rightarrow \tau^+\tau^+\tau^-\tau^-$  for these values of  $h_{\tau\tau}$ . The comparison of these limits with the expected cross-section for left-handed  $H_L^{\pm\pm}$  and right-handed  $H_R^{\pm\pm}$  pair production yields 95% confidence level lower limits for any value of the  $h_{\tau\tau}$  coupling on the mass of the  $H_L^{\pm\pm}$  and  $H_R^{\pm\pm}$  bosons of 98.1 and 97.3 GeV/ $c^2$  respectively.

This search slightly improves previous searches for  $h_{\tau\tau} \geq 10^{-7}$  [15], and in addition is extended to the whole range of  $h_{\tau\tau}$ .

$h_{\tau\tau}$	Left-handed		Right-handed	
	Observed	Expected	Observed	Expected
$\geq 10^{-7}$	99.6	99.6	99.1	99.1
$4 \cdot 10^{-8}$	98.1	98.4	97.3	97.6
$10^{-8}$	99.0	99.4	98.4	98.9
$\leq 10^{-9}$	99.6	99.6	99.3	99.3

Table 4: Median expected and observed limits at 95% C.L. for different values of the  $h_{\tau\tau}$  coupling.

## 5 Conclusion

A search for pair-produced doubly charged Higgs bosons was performed using the data collected by DELPHI at LEP at centre-of-mass energies from 189 GeV to 208 GeV in R-parity conserving supersymmetric left-right symmetric models. Three different analyses were applied to cover the whole range of the  $h_{\tau\tau}$  coupling: decays very close to the interaction point, inside the tracking detectors or beyond them. No significant excess was observed and a lower limit on the doubly charged Higgs mass of 97.3 GeV/ $c^2$  has been set at 95% confidence level for any value of the  $h_{\tau\tau}$  coupling. The limits at 95% confidence level for different values of  $h_{\tau\tau}$  are summarized in table 4. Figure 4 shows the 95% confidence level upper limits on the  $H^{++}H^{--} \rightarrow \tau^+\tau^+\tau^-\tau^-$  pair production cross-section at  $\sqrt{s}=206.7$  GeV for these values of  $h_{\tau\tau}$ .

## Acknowledgements

We are greatly indebted to our technical collaborators, to the members of the CERN-SL Division for the excellent performance of the LEP collider, and to the funding agencies for their support in building and operating the DELPHI detector.

We acknowledge in particular the support of

Austrian Federal Ministry of Science and Traffics, GZ 616.364/2-III/2a/98,

FNRS-FWO and IWT, Belgium,

FINEP, CNPQ, CAPES, FUJB and FAPERJ, Brazil,

Czech Ministry of Industry and Trade, GA CR 202/96/0450 and GA AVCR A1010521,

Danish Natural Research Council,

Commission of the European Communities (DG XII),

Direction des Sciences de la Matière, CEA, France,

Bundesministerium für Bildung, Wissenschaft, Forschung und Technologie, Germany,

General Secretariat for Research and Technology, Greece,

National Science Foundation (NWO) and Foundation for Research on Matter (FOM),

The Netherlands,

Norwegian Research Council,

State Committee for Scientific Research, Poland, 2P03B06015, 2P03B1116 and SPUB/P03/178/98,

JNICT-Junta Nacional de Investigação Científica e Tecnológica, Portugal,

Vedecka grantova agentura MS SR, Slovakia, Nr. 95/5195/134,

Ministry of Science and Technology of the Republic of Slovenia,

CICYT, Spain, AEN96-1661 and AEN96-1681,

The Swedish Natural Science Research Council,

Particle Physics and Astronomy Research Council, UK,

Department of Energy, USA, DE-FG02-94ER40817.

## References

- [1] J.F. Gunion, H.E. Haber, G.L. Kane and D. Dawson, The Higgs Hunter's Guide, Frontiers in Physics, Lecture Notes Series, Addison Wesley, 1990;

- C. S. Aulakh, A. Melfo and G. Senjanovic, Phys. Rev. **D57** (1998) 4174;  
 Z. Chacko and R. N. Mohapatra, Phys. Rev. **D58** (1998) 15003.
- [2] M. L. Swartz, Phys. Rev. **D40** (1989) 1521;  
 K. Huitu et al., Nucl. Phys., **B487** (1997) 27.
- [3] OPAL Collaboration, P. D. Acton et al., Phys. Lett. **B295** (1992) 347.
- [4] DELPHI Collaboration, P. Aarnio *et al.*, Nucl. Instr. and Meth. **A 303** (1991) 233.
- [5] DELPHI Collaboration, P. Abreu *et al.*, Nucl. Instr. and Meth. **A 378** (1996) 57.
- [6] T. Sjöstrand, *PYTHIA 5.719 / JETSET 7.4*, Physics at LEP2, eds. G. Altarelli, T. Sjöstrand and F. Zwirner, CERN 96-01 (1996) Vol 2, 41.
- [7] E. Accomando and A. Ballestrero, Comp. Phys. Comm. **99** (1997) 270.
- [8] F.A. Berends, P.H. Daverveldt, R. Kleiss, Comp. Phys. Comm. **40** (1986) 271, 285 and 309.
- [9] S. Jadach, B.F.L. Ward, Z. Was, Phys. Lett. **B449** (1999) 97;  
 S. Jadach, B.F.L. Ward, Z. Was, Comp. Phys. Comm. **130** (2000) 260.
- [10] S. Jadach, B.F.L. Ward, Z. Was, Phys. Lett. **390** (1997) 298.
- [11] S. Jadach, W. Placzek, B.F.L. Ward, Comp. Phys. Comm. **79** (1994) 503.
- [12] DELPHI Collaboration, Search for supersymmetric particles in light gravitino scenarios, EP Paper 299/Draft 1.
- [13] DELPHI Collaboration, P. Abreu *et al.*, W pair production cross-section and W branching fractions in  $e^+e^-$  interactions at 189 GeV, Phys. Lett. **B479** (2000) 89.
- [14] A.L. Read, in CERN Yellow Report 2000-005, p. 81.
- [15] OPAL Collaboration, G. Abbiendi et al., Phys. Lett. **B256** (2002) 221-232.



# DELPHI

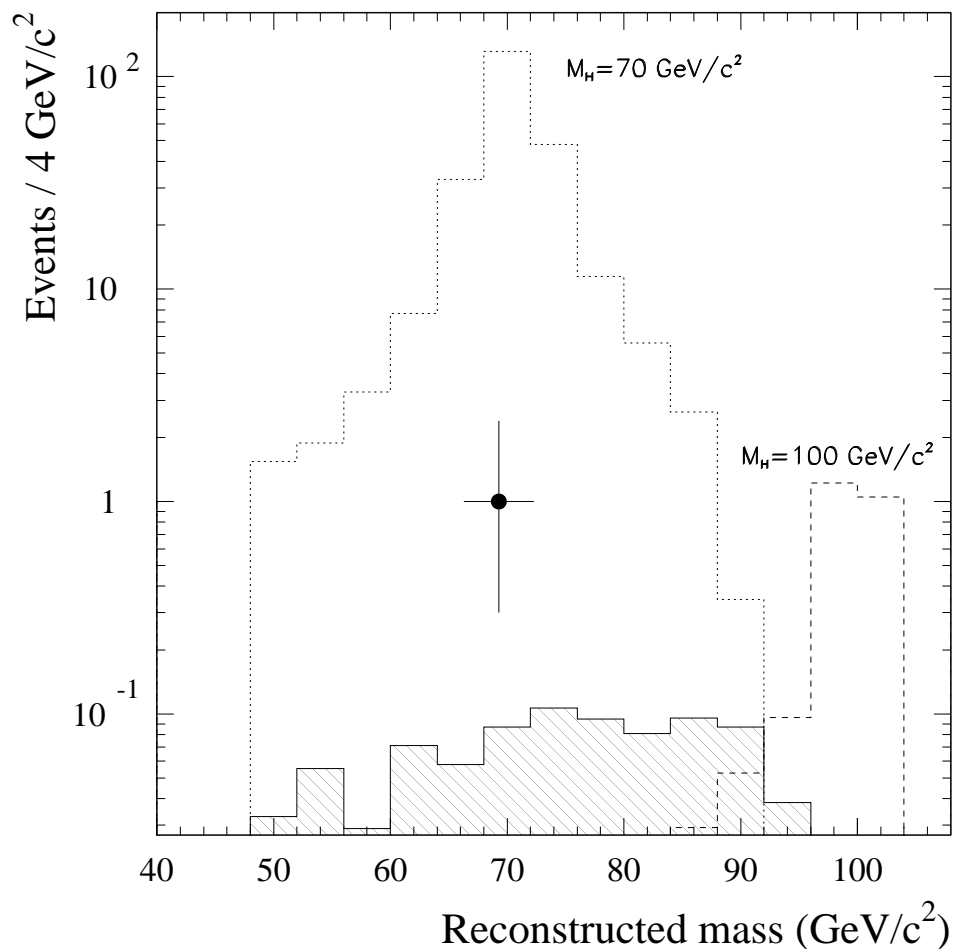


Figure 1: The reconstructed mass distribution after all cuts for the small impact parameter search. The hatched histogram corresponds to the expected background and the dot with the error bar shows the one remaining candidate event. The dashed line corresponds to simulated events with  $m_{H_L^{\pm\pm}} = 70 \text{ GeV}/c^2$  and the dotted line corresponds to simulated events with  $m_{H_L^{\pm\pm}} = 100 \text{ GeV}/c^2$ .

# DELPHI

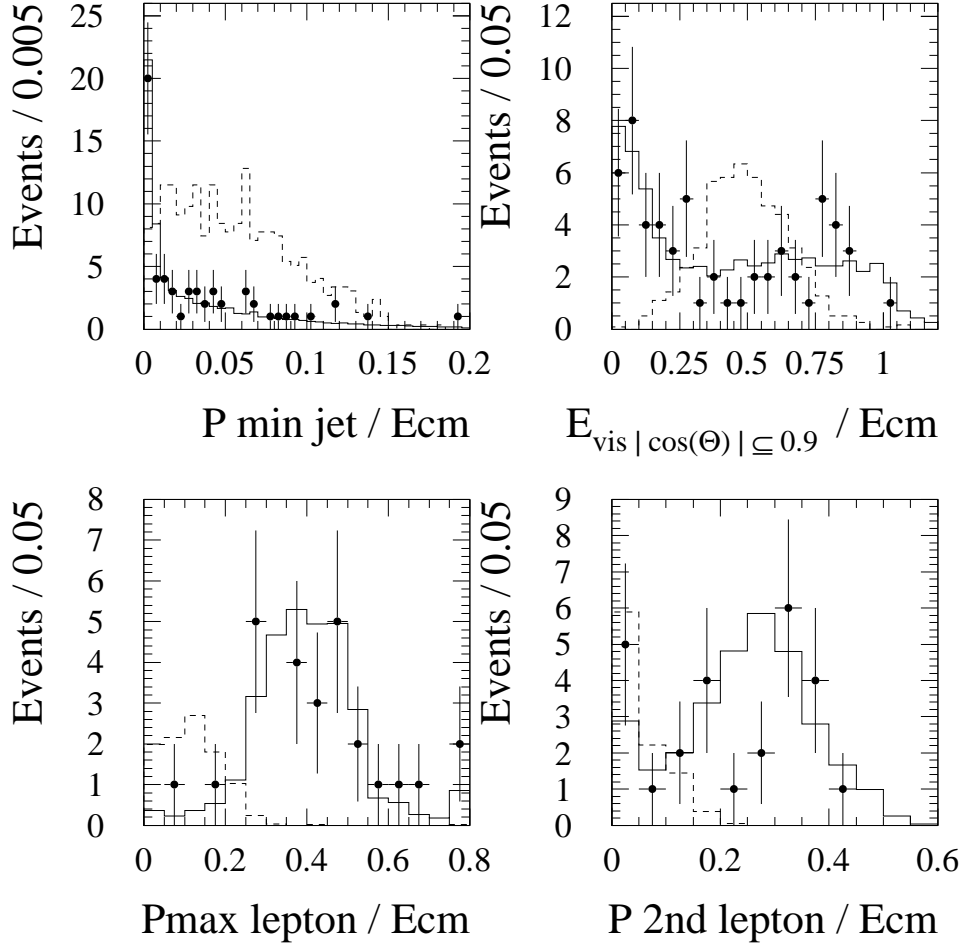


Figure 2: Event selection variable distributions at different stages of the analysis for the small impact parameter search. The top plots show the minimum momentum of the jets and the visible energy outside  $25^\circ$  around the beam pipe scaled by  $\sqrt{s}$  after the four-jet preselection cuts. The bottom plots show the momentum of the most energetic identified lepton and the momentum of the second most energetic identified lepton scaled by  $\sqrt{s}$  after the anti- $\gamma\gamma$  cuts. The solid lines show the expected background, the dots the observed data and the dashed lines correspond to  $m_{H_L^{\pm\pm}} = 100 \text{ GeV}/c^2$  in arbitrary units.

# DELPHI

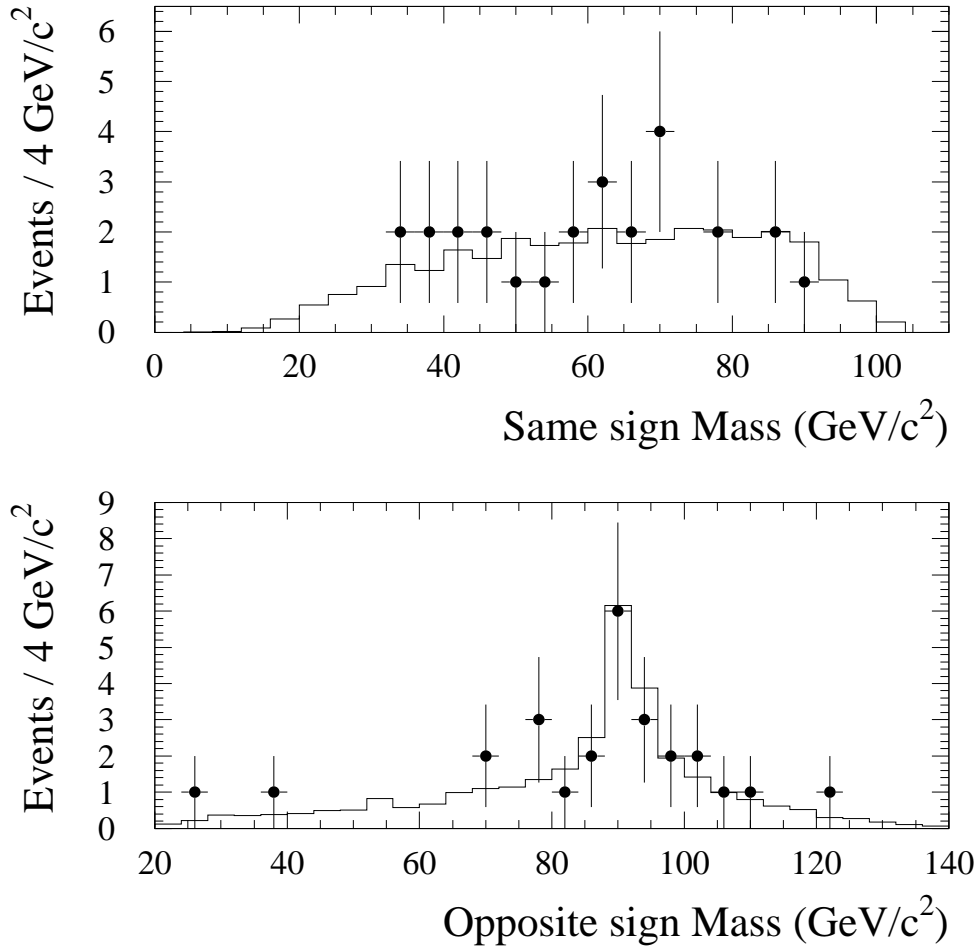


Figure 3: Reconstructed mass distributions for the small impact parameter search. The masses are shown for the same sign lepton pairs (top) and the opposite sign lepton combination closest to the Z mass (bottom). These distributions are shown before the anti four lepton cuts. The solid lines show the expected background and the dots the observed data.

# DELPHI

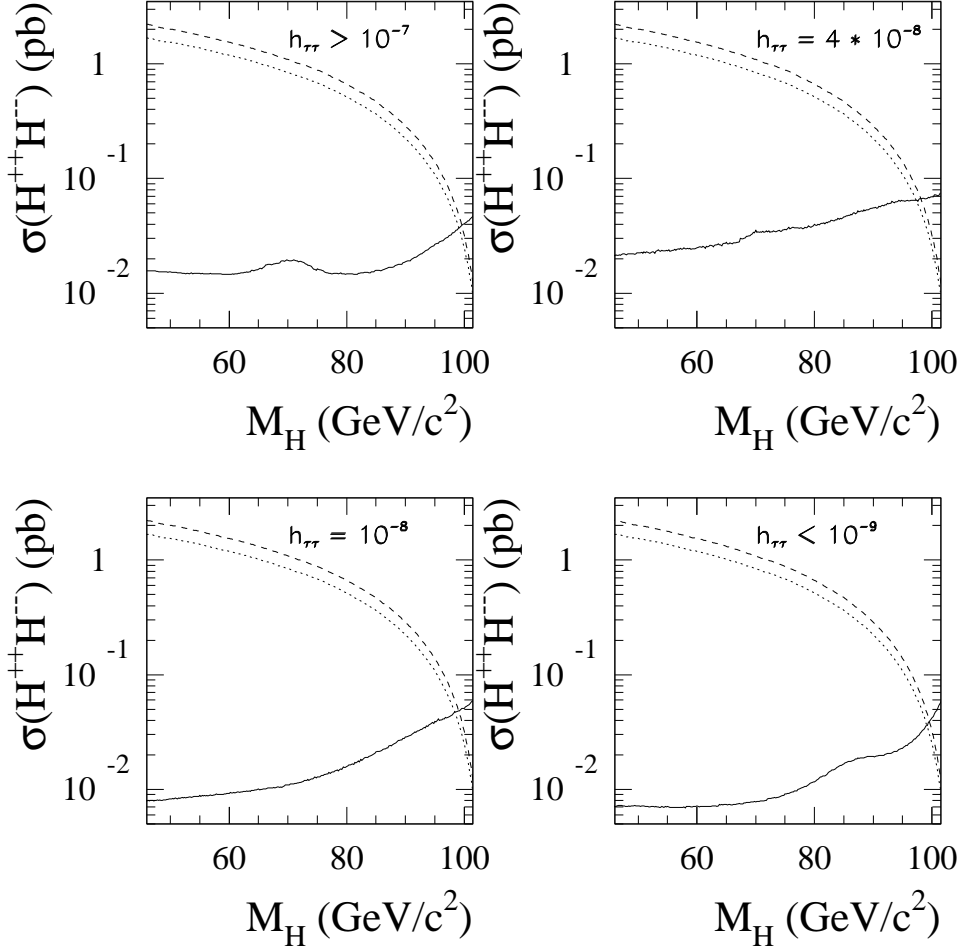


Figure 4: The solid line shows the 95% confidence level upper limit on the  $H^{\pm\pm}$  pair production cross-section at  $\sqrt{s}=206.7$  GeV assuming 100% branching ratio for the decay of  $H^{\pm\pm}$  into  $\tau^{\pm}\tau^{\pm}$  for different values of  $h_{\tau\tau}$ . The dashed and dotted lines show the expected production cross-section of  $H_L^{\pm\pm}$  and  $H_R^{\pm\pm}$  pairs in left-right symmetric models.